Desalination and Water Treatment
www.deswater.com

doi: 10.5004/dwt.2021.27070

222 (2021) 36–46
May

Experimental study on the deaeration process of low temperature thermal desalination plant

D. Balaji*, G. Dhinesh, S.V.S. Phani Kumar, M.V. Ramana Murthy

Ocean Structures Department, National Institute of Ocean Technology, Chennai, India, Tel. +91 44 66783349; Fax: +91 44 66783580; email: dbalaji@niot.res.in (D. Balaji), Tel. +91 44 66783564, email: dhinesh@niot.res.in (G. Dhinesh), Tel. +91 44 66783353; email: phani@niot.res.in (S.V.S. Phani Kumar), Tel. +91 44 66783586; email: mvr@niot.res.in (M.V. Ramana Murthy)

Received 28 July 2020; Accepted 20 January 2021

ABSTRACT

Low temperature thermal desalination process uses an unique technology in which the surface seawater (28°C–29°C) is flash evaporated inside a vacuum flash chamber maintained at a pressure of 25–27 mbar (abs) and resultant vapour is condensed in the condenser using deep-sea cooling water at 12°C–13°C drawn approximately from 350 to 400 m depth. The objective of the present paper is to discuss the effort that has been made to improve the deaeration process using a row of tube bundles with different pitch ratios such as 1.25, 1.5, 2, and 3 which were placed in the entry seawater passage pipeline to the deaerator. Tube bundle is expected to create disturbance in the water and improve the deaeration of dissolved gases (non-condensable; NC). Influence of these tube bundles on the assessment of NC gases release rate is discussed in the present work. A new methodology with two equation model has been developed to determine the deaeration efficiency based on the experimental study is presented in this work. It is observed from the study that the amount of NC gases released from the seawater by bundles influences the escape rate of water vapour from the main condenser. A maximum of 86.4% deaeration efficiency is observed from the experiments.

Keywords: Deaeration efficiency; LTTD plant; Dissolved gas; Tube bundle pitch ratio; Water vapour escape rate

1. Introduction

Water and food security are vulnerable in the continuously changing climatic patterns due to the global warming [1]. The gradually changing climatic conditions create irregularity in the seasonal rainfall in almost all parts of the world, increasing the demand for the quality water in most of the tropical countries such as India. The dependence on the rivers, lakes, and ground water traditionally satisfied the daily water needs in tropical countries fed by seasonal rainfall of the country. But, the rapid population growth and urban development affected the catchment areas for these water sources, increasing the demand for potable water.

Many sophisticated desalination technologies have been developed in the last few decades for producing potable drinking water from seawater. Conventional desalination processes are being used by the most of the developed and under developing countries for meeting their water needs. The conventional operating methods are generally divided in to two: membrane based and thermal based desalination technologies. Traditional method is distillation which involves boiling of seawater and re-condensation of the evaporated water vapour leaving the salt impurities in the reject water. The membrane based process includes the seawater reverse osmosis (SWRO) and electrodialysis (ED), whereas the thermal based process includes multi-stage

* Corresponding author.

flash (MSF) evaporation, multi-effect distillation (MED), and mechanical vapour compression (MVC).

MSF units are mostly used in the Middle East countries. It is one type of thermal desalination process. It is designed with either once through flow system or brine re-circulation flow system. The once through flow system of MSF unit generally divided into two sections: brine heater section and heat recovery section. If it is a brine re-circulation flow system MSF unit then heat rejection section to be added in addition. A lower vacuum pressure is maintained successively in the stages of MSF unit. This would maximize water and energy recovery. Either steam ejector or mechanical vacuum pump is being used to create vacuum in the stages of the flash evaporator. In order to increase the performance of the MSF unit, some portion of the brine discharge water is re-circulated by mixing with incoming seawater. A portion of seawater is obtained as product water and remaining is rejected as brine water at high total dissolved solids (TDS).

MED is one of the important and oldest desalination technologies in use. In this technology, evaporation takes place in the series of evaporative chambers with a successive decrease in the pressure and temperature in consecutive stages. In each evaporative chamber, the seawater is sprayed through nozzles over the horizontal tube bundles and simultaneous passage of heating steam inside the tubes of the bundles. On the external portion of the tubes, a liquid film flows over the tubes and evaporates a portion of it by absorbing a heat from the steam. Using this steam from the power plant, the evaporation occurs in the first stage of the MED unit. The vapour generated in the first stage from the seawater goes into the tube of the second stage evaporator as a steam to evaporate the seawater sprayed on the outer surface of the tube. This process is repeated in the stages of the evaporator given in the MED unit.

MVC uses a mechanical compressor to produce heat by compressing vapour to evaporate the seawater. The compressor develops vacuum inside the evaporator and compresses the water vapour generated from the evaporator and then condenses it inside the bundle of the tubes. Seawater is allowed to fall on the outside of the heated horizontal tubes. Portion of the seawater evaporates and produces vapour while the heated water vapour condenses inside the horizontal tubes.

RO is a process in which the water from pressurized seawater is separated from the dissolved saline impurities by passing through a semi-permeable membrane without the application of heat or phase change. It is a process in which the solvent is forced from a region of high solute concentration to a region of low solute concentration through the semi-permeable membrane by the application of pressure in excess of osmotic pressure. In this process, the natural movement of water particle is reversed by the application of pressure against osmotic pressure. A typical large seawater RO plant consists of five major items such as intake seawater system, seawater pre-treatment system, high pressure plunger pumping system, RO membranes with modules, and finally post-treatment system.

ED is an electro-chemical separation process that uses electrically charged ion-exchange membranes with an electrical potential difference as a driving force [2]. It depends on the fact that most of the salt particles dissolved in seawater are ionic. They are either positively charged (cationic) or negatively charged (anionic) ions. They travel towards electrodes with an opposite electric charge. Membranes are used or constructed to permit the selective passage of either cations or anions [2].

The latest development in new RO membrane materials is discussed in this section. The polymeric materials include aromatic polyamides, polybenzimidazole, polyphenylene oxide, hydrated metal oxides, cross-linked and blended cellulose acetates, cross-linked polyvinylpyrrolidone, and cross-linked polyethylenimine [3]. Cellulose based membrane includes cellulose acetate, cellulose diacetate, cellulose triacetate, and piperazine. Thin film composite membrane includes polysulfone, polyimide, polypropylene, polyketone, and polyethylene terephthalate. Ceramic membrane includes alumina, zirconia, and titania. Carbon based membrane includes ordered mesoporous materials, carbon nanotubes, single-walled carbon nanotubes, double-wall carbon nanotubes, multi-walled carbon nanotubes, and graphene oxide membranes [4].

Hybrid thermal desalination process includes two or more desalination technologies in order to harness the comparative advantages of these technologies. Hybrid desalination includes membrane distillation (MD) and reverse osmosis combined with forward osmosis, MSF evaporation or MED. Other hybrid thermal desalination includes the integration of the MED with conventional process with an adsorption cycle in order to extend the operating range of the temperature of the conventional MED plant [5]. Hybrid desalination collectively increases the operational reliability and recovery. It is reported that MSF water production cost is reduced by 17%–24% by hybridization of the RO with MSF unit [6]. It is also reported that MSF–RO hybrid performance combined with nuclear power plant increases water production when MSF condenser cooling water given as feed to the RO plant [7].

MD is a thermally driven; membrane-based process combines the use of distillation and membranes. The temperature difference is maintained between the supply solution which comes in contact with membrane in one side and the space in the other side of the membrane. The temperature difference leads to the difference in vapour pressure. This in turn led to the production of vapour through membrane. This vapour gets condensed to form product water upon touching the coolant side of the membrane. The membranes are hydrophobic in nature which allows only vapour to pass through it [2].

The reason to choose low temperature thermal desalination (LTTD) process rather than the conventional desalination processes is that the LTTD technology is most suitable for desalination plant at Islands where the depth of the sea to draw cooling seawater comes nearer to the shore in the range of 500–800 m. This is not possible in the mainland due to long distance from shore to reach that depth where the cooling water is available at 12–13°C. The technologies such as RO, MED, MSF entail the challenges such as disposal of highly saline or high temperature reject water into the shallow coasts, and safe guarding the marine living organisms. In this perspective, the LTTD technology [8] developed by National Institute of Ocean Technology is one of the promising technology that uses ocean thermal

gradient which do not affect the ecosystem. Currently, three 100 m^3/d capacity LTTD plants are operating in Kavaratti, Minicoy, and Agatti Islands and one 150 m^3/d capacity LTTD plant operating in Kalpeni Island of UT Lakshadweep, India, satisfying the drinking water needs of local communities. Low operating temperature, no chemical additives, low maintenance, and no life threat to ecosystem are some of the advantages of the LTTD plants.

For a thermal desalination plant, evacuating the non-condensable (NC) gases and air leak into the process equipment of the LTTD plant [9] is very essential for maintaining the fresh water production capacity of the plant. Vacuum system alone consumes around 31% of total energy demand of the LTTD plant. Vacuum system evacuates gases such as NC gases, air leakage, and uncondensed escape water vapour from the main condenser and evaporator and to sustain the required saturation pressure inside the equipment. Oxygen and nitrogen present in abundant quantity in seawater compared to other dissolved gases. CO_2 present mostly in the form of carbonic acids. The factors such as temperature of seawater, salinity of seawater, biological processes, ocean currents, and mixing processes affects the quantity of dissolved gases present in the seawater.

The amount of NC gases quantity depends on the mass flow rate of feed water enters into the process equipment. The amount of the NC gases released into the evaporator may affect the thermal performance of the desalination process. Because these NC gases would wrap the outside surface of heat transfer tubes and act as a thermal insulator between the water vapour and condensate film on the tube surface that lead to decreased condensation rate. This resulted in increased escape water vapour rate and hence the vacuum load. Therefore, the amount of NC gas present in the condenser considered to be the most influential parameter that decides the amount of vapour escape rate from the condenser. In order to minimize the effect of the NC gases a conical truncated chamber called deaerator is being used to remove a portion of these gases from seawater before they entering into the flash chamber or evaporator as shown in Fig. 1 with vacuum system connection piping diagram.

The main objective of current study is to discuss about the mechanism adopted to improve and assess the deaeration of NC gases in the deaerator by creating turbulence in the intake feed water in the pathway of the deaerator using rows of tubes with different pitch ratios such as 1.25, 1.5, 2, and 3 and improve the performance of the LTTD process. Enhancement of deaeration is assessed by means of deaeration efficiency and escape water vapour rate measured from the intermediate condenser of vacuum system.

2. Deaeration in thermal desalination systems

Amount of NC gas presence depends on the temperature of seawater (29°C) at which it is supplied to the plant. Amount of these gases released inside the process equipment depends upon the mass flow rate of feed water. It is reported in the literature that even 1% wt. by volume of NC gas has the ability to reduce the heat transfer co-efficient by 50% [10]. It is observed from the experiment in LTTD plant that the increase in NC gas flow rate increased the water vapour escape rate which is equivalent to 60.4% of the total vacuum load [11]. It is estimated that NC gas content in the seawater would be in the range of 14–16 mg/L [12–14] and it goes maximum up to 19.2 mg/L [15,16]. The percentage of the NC gases in the generated vapour flow rate is in the range of 0.19%–0.27% corresponding to the maximum feed water flow rate (648 ton/h) that enters the evaporator for the Agatti LTTD plant. Even though its contribution on the vacuum load is found to be less compared to escape water vapour, still it plays a major role in increasing the escape rate of water vapour, due to the resistance given by NC gases to heat transfer between water vapour and condensate film formed on the outer surface of the cooling tubes. Solubility of oxygen in water at different temperatures and pressure is depicted in Fig. 2. Amount of NC gases dissolved in the seawater depends on two laws namely Henry's law and Raoult's law.

Henry's law states that at constant temperature the volume of gas dissolved in the water is directly proportional to the partial pressure of that gas acting on the liquid surface. It is given in mathematical form as follows:

$$p = k_H \times C \tag{1}$$

where p is the partial pressure of the gas above the solution, C is the concentration of the dissolved gas, and k_H is Henry's constant that depends on the solute, the solvent, and the temperature.

Raoult's law states that the partial pressure of the each component of an ideal mixture of liquids is equal to the vapour pressure of the pure component multiplied by its mole fraction in the mixture. Its mathematical form is given as follows:

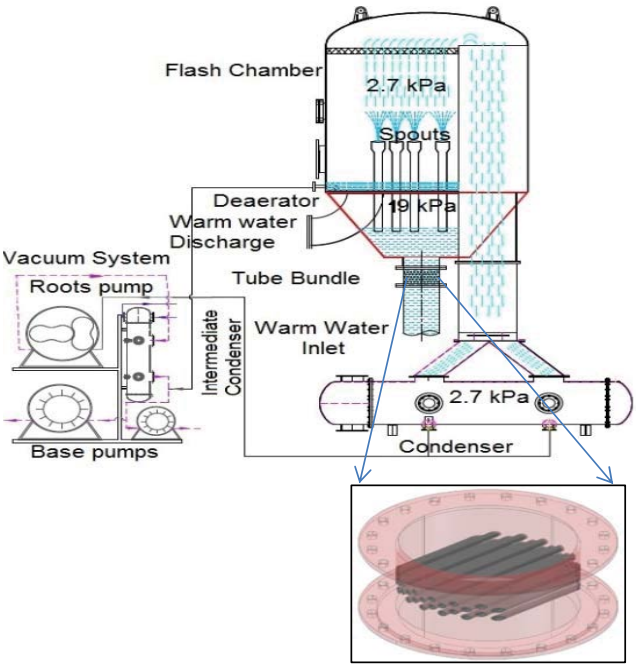

Fig. 1. A sketch of deaerator and flash chamber connected to vacuum system.

$$p_i = p_i^* x_i \quad (2)$$

where p_i is the partial pressure of the component i in the gaseous mixture above the solution, p_i^* is the vapour pressure of the pure component i, and x_i is the mole fraction of the component i, in the mixture in the solution.

Capacity of the vacuum depends on the escape vapour rate as well as the temperature and mass flow rate of cooling water circulated inside the condenser tubes. Design of pumping capacity of the vacuum system also influences the amount of vapour escapes from the surface condenser. It is reported that the 100 times variation is possible in the overall heat transfer co-efficient of the condenser even if a small quantity of NC gases are present in the shell portion of the condenser [17].

Pumping speed of the vacuum system is estimated using Eq. (3) by suitably assuming leakage of air at 4 kg/h based on the the volume under the vacuum [18] and with the experience from the Kavaratti LTTD plant, the vapour escape rate is taken as 0.3% of the water vapour generation rate for determining the vacuum load and it is worked out to be around 2,000 m^3/h at a suction pressure of 15 mbar. The volumetric load ($\dot{V}$) on the vacuum system is obtained from the suction pressure, P, temperature, T, and mass flow rates of escaping water vapour ($\dot{m}_{vap}$), NC gases ($\dot{m}_{NC}$), and air leakage ($\dot{m}_{air}$) by using Eq. (3)

$$\dot{V} = \left[\frac{RT}{P}\right]\left[\frac{\dot{m}_{vap}}{M_{vap}} + \frac{\dot{m}_{NC}}{M_{NC}} + \frac{\dot{m}_{air}}{M_{air}}\right] \quad (3)$$

where R is the universal gas constant.

Break up of the vacuum load is shown in Table 1 which indicates that the major portion of load is contributed by the water vapour escape rate. Due to tidal and cooling water temperature variation at the site, the actual vacuum load varies from the designed load. First stage compression is achieved by the liquid ring base pumps followed by roots pump which completes second stage compression and bring down operating pressure up to 27 mbar. An intermediate condenser maintains the required pressure in the flash chamber and the condenser by condensing vapour escapes from process condenser as shown in Table 1.

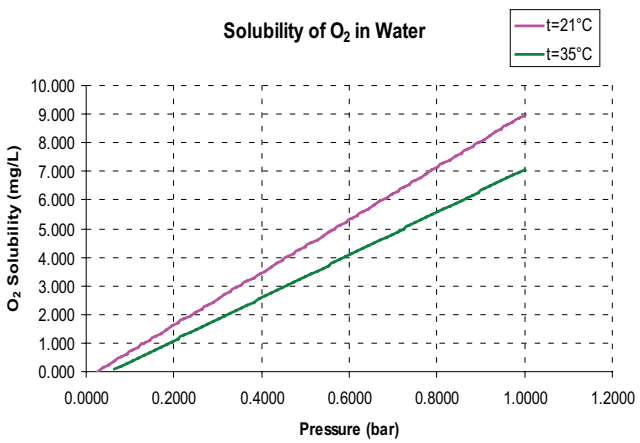

Fig. 2. Solubility of O_2 in water.

3. Description of the experiment and the measurement procedure

A portion of NC gases dissolved in the seawater will be released out when exposed to low pressure zone inside the deaeration chamber. Deaerator and flash chamber are connected by vertical spout pipes, 1.6 m long and 24 in number. Feed intake seawater from caisson enters the deaerator passes through the spout pipes 0.1 m in diameter and then flashes inside flash chamber. The spouts are designed for the dual purposes of provision of an elevated surface for warm water as it enters the flash chamber that is immediately exposed to its operational pressure; and, maintenance of a differential pressure between the flash chamber and the deaerator. The diameter of the spouts determines the velocity of water entry into the flash chamber and the length of the spout and its immersion inside the fluid in the deaerator determine the operating pressure inside the deaerator.

During operation, the flash chamber is maintained at 24–27 mbar and the deaerator pressure is observed to vary between 150 and 190 mbar. Vacuum system picture is shown in Fig. 3. Flow obstruction, in terms of a tube bundle with different pitch ratios such as 1.25, 1.5, 2, and 3 are placed in the warm water piping as shown in Fig. 4 at deaerator entry to study the deaeration and release of NC gases. As the local pressure reduces in the warm water path, the dissolved gases tend to separate from the water. The gases thus separated settle at the top of the deaerator chamber while the water directly passes into the flash chamber. A port provided at the top of the deaerator helps evacuating the collected gases to the liquid ring vacuum pump that is operating at a pressure higher than

Table 1
Estimated vacuum load at operating conditions

Item descriptions	Details
Plant capacity	100 m^3/d
Saturation temperature	22.5°C
Saturation pressure	27 mbar
Minimum operating pressure at booster entry	15 mbar
Warm water inlet temperature	28°C
Cold water inlet temperature	12°C
Warm water flow rate	180 kg/s
Cooling water flow rate	150 kg/s
Water vapour escape	1,270 m^3/h @ 18 kg/h
Non-condensable gas	478 m^3/h @ 12 kg/h
Air leakage rate	252 m^3/h @ 4 kg/h
Total vacuum load	2,000 m^3/h @ 34 kg/h
Stages of compression	2
Roots pump capacity and power	2,000 m^3/h @ 5.5 kW
Base pump capacity and power	400 m^3/h @ 13.2 kW

the roots pump. Various configurations of the tube bundles with differing flow obstruction areas are designed, by varying the diameter of the tubes and their pitch.

4. Methodology for analysis

NC gas, uncondensed water vapour escape, and air leak into the system gives load to the vacuum system. Among these, the leakage air, entering from various joints such as instrumentation ports, flange connections, valve stems, etc., in the system under vacuum increases the pressure of the evacuated flash chamber and is assessed by measuring the rate of increase in pressure of an isolated flash chamber left under vacuum for a known period. Empirical relations based on the solubility of oxygen and nitrogen in seawater are used to estimate the amount of gases dissolved in the seawater for a given temperature and pressure. Oxygen and nitrogen gases are considered for the calculation of NC gases, since the presence of these gases in the atmospheric is abundant (99%). For Agatti system, the average leak rate is found to be about 0.22 kg/h, as shown in Fig. 5a and the solubility of oxygen and nitrogen is shown in Fig. 5b.

The water vapour that is escaped from the condenser is heated up in the roots pump and part of it is condensed as it passes through the intermediate condenser that is fed by the reject cold water from the plant. The mass flow rates of leakage air ($\dot{m}_{air}$), dissolved oxygen ($\dot{m}_{O_2}$), dissolved nitrogen ($\dot{m}_{N_2}$), escape vapour ($\dot{m}_{\text{escape vapour}}$), and condensation inside the intermediate condenser ($\dot{m}_{\text{water, intermediate condenser}}$), the pressure, P, and the temperature, T, of the gases in roots pump and base pump are monitored and used in a two equation model to simultaneously solve the deaeration efficiency (h) and the vapour escape rate as shown in Eqs. (4) and (5). The pumping capacities of the base pump and the roots pump are taken as 400 and 2,000 m^3/h, respectively. A flowchart of the algorithm is provided in Fig. 6.

$$\dot{V}_{\text{roots pump}} = \left[\frac{RT}{P}\right]_{\text{roots pump}} \left[\begin{array}{l} \dfrac{\dot{m}_{\text{escape vapour}}}{M_{\text{water}}} + \\ (1-\eta)\left(\dfrac{\dot{m}_{O_2}}{M_{O_2}} + \dfrac{\dot{m}_{N_2}}{M_{N_2}} + \dfrac{\dot{m}_{air}}{M_{air}}\right) \end{array}\right] \tag{4}$$

$$\dot{V}_{\text{base pump}} = \left[\frac{RT}{P}\right]_{\text{base pump}} \left[\begin{array}{l} \dfrac{\dot{m}_{O_2}}{M_{O_2}} + \dfrac{\dot{m}_{N_2}}{M_{N_2}} + \dfrac{\dot{m}_{air}}{M_{air}} + \\ \dfrac{\dot{m}_{\text{escape vapour}}}{M_{\text{water}}} - \dfrac{\dot{m}_{\text{water, intermediate condenser}}}{M_{\text{water}}} \end{array}\right] \tag{5}$$

5. Estimation of deaeration efficiency and vapour escape rate

Graphs of the estimated deaeration efficiency and the vapour escape rates for the system with four different configurations of the tube pitch ratios such as 1.25, 1.5, 2, and 3 of the inserted obstructions are shown in Figs. 7a–d with respect to the time the plant is operated. The data plotted is from the startup to shutdown of the plant

Fig. 3. Vacuum system in Agatti.

Fig. 4. Tube bundle with different pitch ratio.

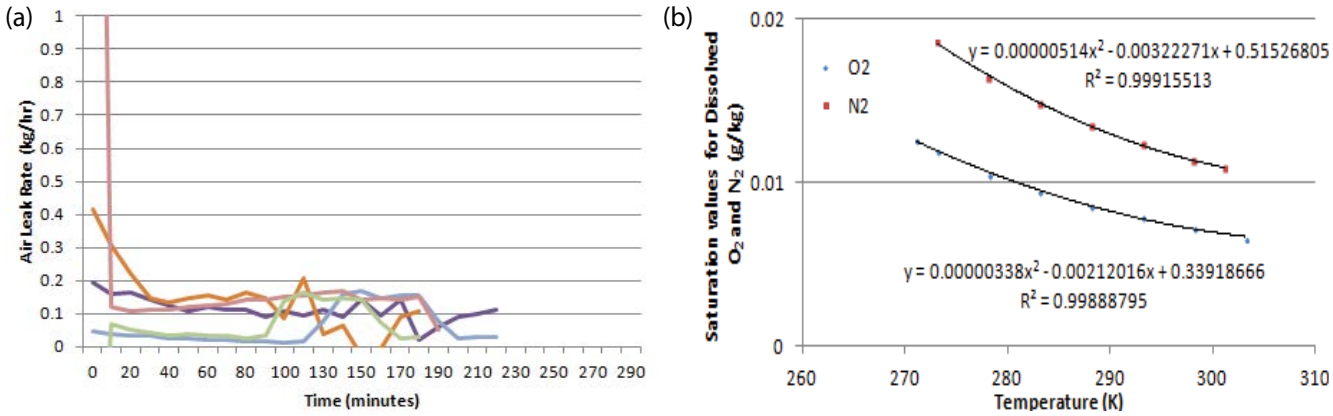

Fig. 5. (a) Leak rate of Agatti flash chamber–condenser system. (b) Solubility of oxygen and nitrogen in seawater as a function of water temperature.

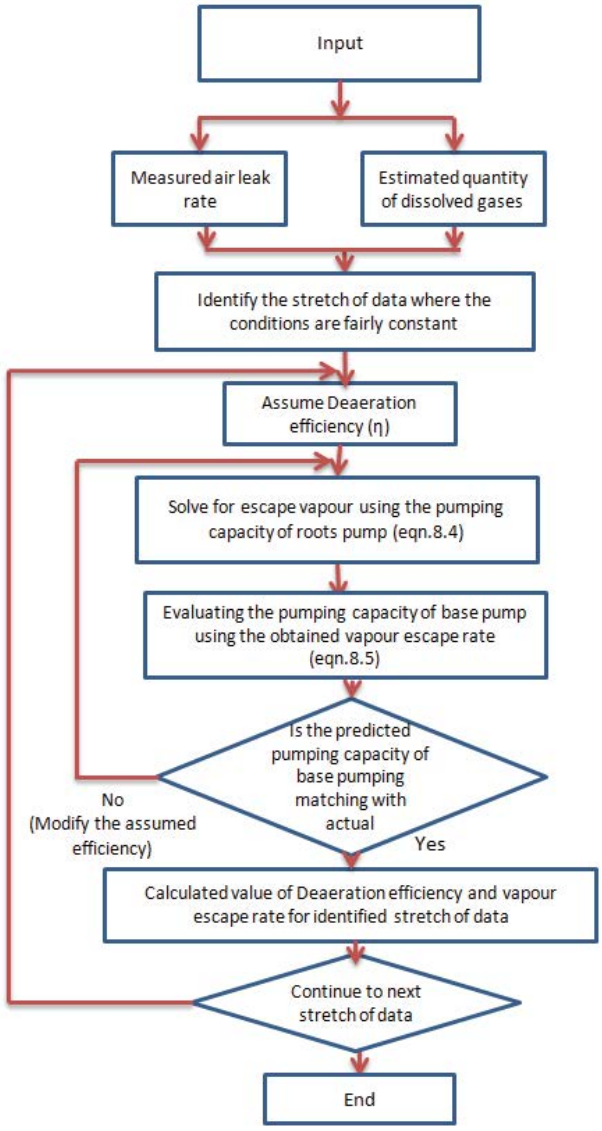

Fig. 6. Flowchart showing methology of analysis of deaeration efficiency.

for different days with deaerator connected to the second stage of the vacuum system. It is observed that the deaeration efficiency of the system varies continuously. Decrease in deaeration efficiency was observed during the plant operation, during this period, the warm water flow rate was observed to be continuously decreasing with the passage of time. This could be due to the fact that the deaerator could not able to handle the NC gas load coming from the horizontal intake half filled seawater pipeline lying on the bridge during low tide. As a result, NC gases escapes in to the flash chamber through spout pipe, which is discussed below. From Eq. (4), the deaeration efficiency (h) could be defined as the fraction of the leakage air and dissolved gases removed by the deaerator.

As mentioned above, the decrease of deaerator efficiency possibly could be due to two scenarios, such as, when the deaerator is filled up with the removed gases and the pressure of these collected gases pushes the water level to escape into the flash chamber, or, when excess air enters the deaerator and in turn enters the flash chamber. It was observed that the deaerator pressure increased steadily from the startup time of the plant to reach a value of 192 mbar. Considering a pressure of 27 mbar inside the flash chamber and a height of 1.65 m of the spouts, 192 mbar would be the maximum pressure that could be sustained by the deaerator section before the water sealing for the spouts breaks and gases from the deaerator enter the flash chamber, as shown in Fig. 8.

Water vapour escape load was estimated to be as high as 1,700 m^3/h with a corresponding roots pump suction pressure of 15 mbar, indicating about 85% of the roots pump capacity being exhausted by the escape water vapour. Since the measured air leak rate of the system (0.22 kg/h) was found to be about 5% of the value specified by the Heat Exchange Institute standard and also since a portion of the NC gases is trapped in the deaerator, the lower suction pressure of the roots pump and higher water vapour escape rate would mean that the pumping capacity of the vacuum system is in excess of the required capacity. The plant was operated by isolating 25% capacity of the base vacuum pump (2.2 kW) from the vacuum system, which increased the roots pump suction pressure to 19 mbar while maintaining

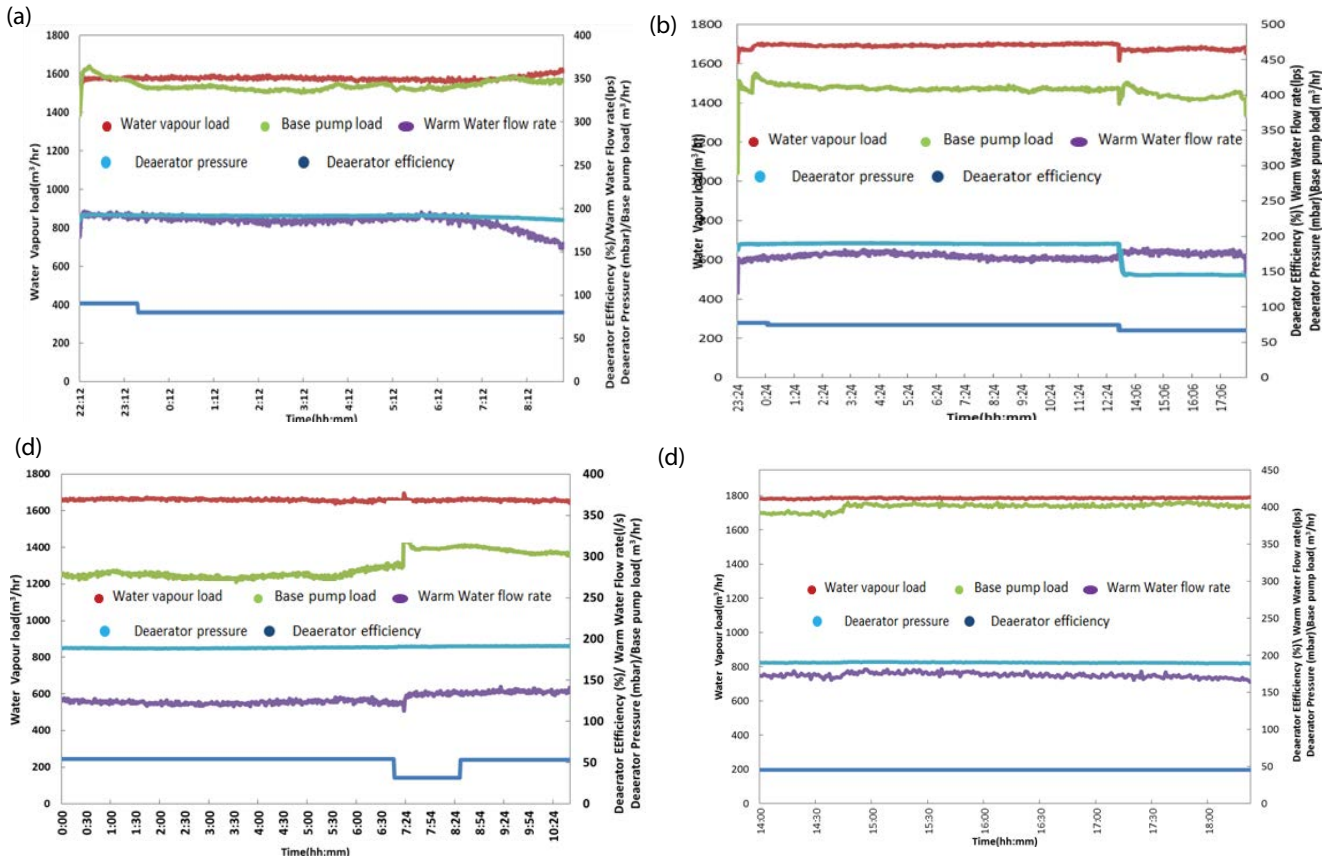

Fig. 7. Plots of the estimated deaerator efficiency for the plant with different pitch ratios are (a) 1.25, (b) 1.5, (c) 2, and (d) 3.

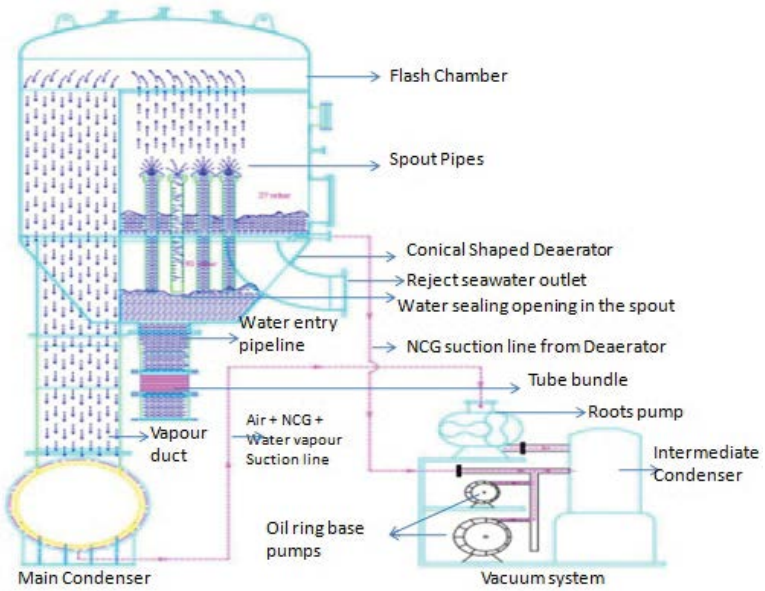

Fig. 8. A sketch of the deaerator–flash chamber showing a break in the water sealing of the spout pipes.

almost same fresh water production rate (Figs. 9a–d). The isolation of vacuum pump resulted in a reduction of 16% of power consumption of vacuum system and 5% of total power consumption of the plant.

Water vapour load depends on factors such as warm water flow rate, cold water flow rate, cooling water temperature, and NC gas presence in the condenser. Distinct slopes of water vapour load and NC gas load are observed

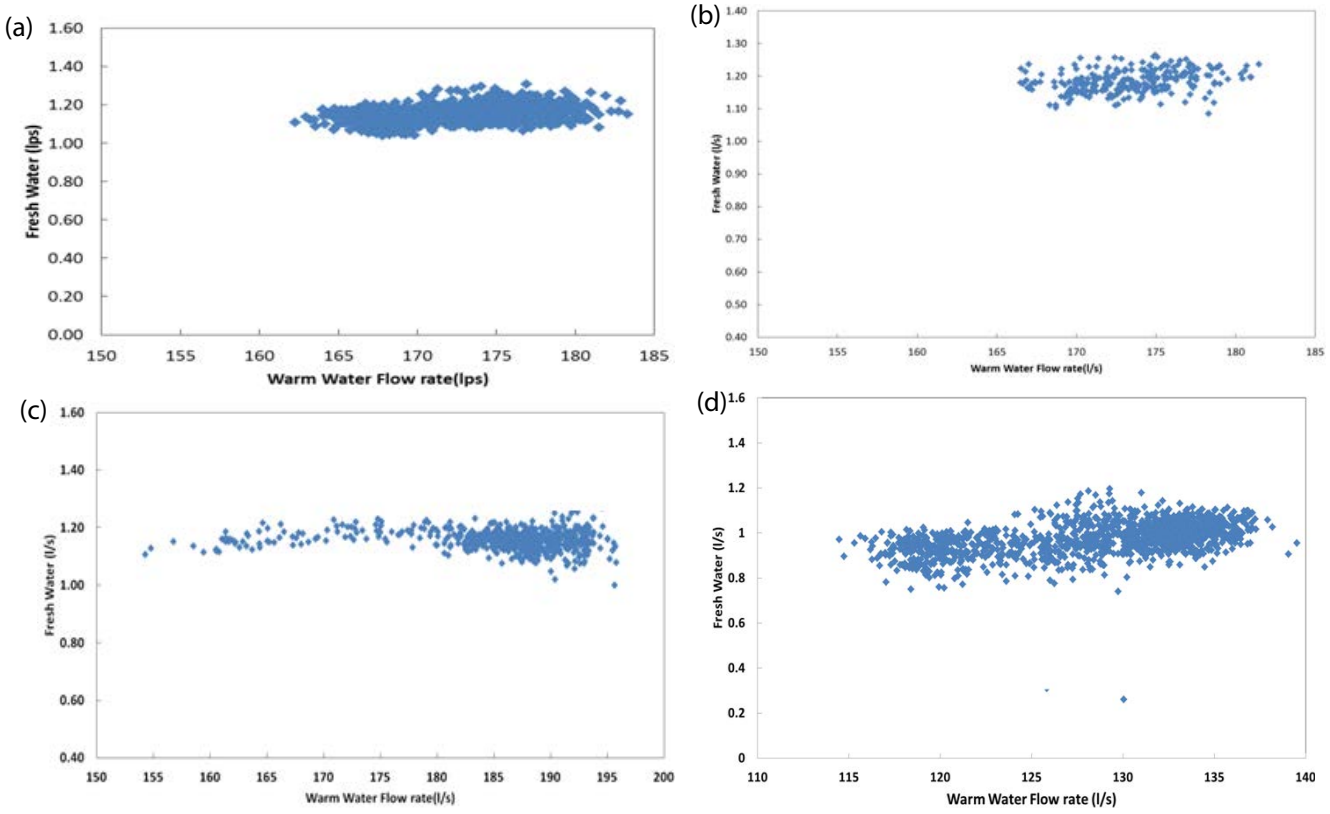

Fig. 9. Warm water flow rate vs. fresh water production rate with different pitch ratios are (a) 1.25, (b) 1.5, (c) 2, and (d) 3.

for different warm water flow rates as shown in Figs. 10a–d and 11a–d, respectively, corresponding to different pitch ratios. Efficiency of deaerator corresponding to the warm water flow rate for different tube bundles is shown in Fig. 12. It is observed that the deaeration efficiency varies between 2% and 85%. Tube pitch ratio 1.25 is found to be having higher deaeration efficiency than the other tube bundles due to better disturbance of liquid flow compared to other configurations. It is also observed that the period of prediction of the low efficiency of deaeration coincided with the occurrence of low tide in the region. It is also observed that the booster pump suction pressure recorded lowest value of 14 mbar during plant operation as shown in Fig. 13.

An inspection of the piping layout of the Agatti plant revealed that a portion of the warm water pipe could lie above the warm water pump shut-off head, for a portion of the lowest low tides, creating a void in the pipeline for the NC gases to accumulate and also causing a drop in the warm water flow. When the accumulated gases travel along the pipeline on the bridge and reach the deaerator, they are seen in the deaerator as an additional load. The performance of the deaerator during this period is decreasing. It is observed from Fig. 12 that the maximum deaeration efficiency achieved in the deaerator is 86.4%, which coincided with the theoretical limit, as explained below:

- Typical average inlet temperature of surface seawater: 28.45°C
- Saturation pressure of water at 28.45°C: 37.81 mbar
- Atmospheric pressure: 1,013 mbar
- Amount of gases dissolved in seawater at the boiling point: 0 ppm
- Amount of O_2 + N_2 dissolved in the seawater at 28.45°C and atmospheric pressure: 19 ppm
- Average pressure of the deaerator: 170 mbar
- Maximum deaeration at about 170 mbar: ((1,013 − 170)/(1,013 − 37.81)) × 100 = 86.4%

The performance parameters of different desalination technologies are given in Table 2.

The specific electrical energy consumption of the different desalination technologies are given in Table 2 [19–21]. In that LTTD technology found to be having high value compared to other desalination technologies. This could be due to the fact that this technology used single stage flash evaporation where the warm surface seawater enters the flash evaporator at 29°C and leaves the evaporator at 24°C, whereas the deep-sea cooling water enters the shell and tube condenser at 12°C and leaves at 17.5°C. LTTD process is operated in the range of 17–18°C only using the ocean temperature gradient. It is not possible to introduce MSF evaporation; as a result the electrical energy consumption is slightly higher for the LTTD technology compared to the other desalination technology. However, LTTD technology possesses certain advantages which are not available in the other conventional desalination technologies such as easy operation and maintenance, negligible increment in the TDS of the reject water from flash evaporator

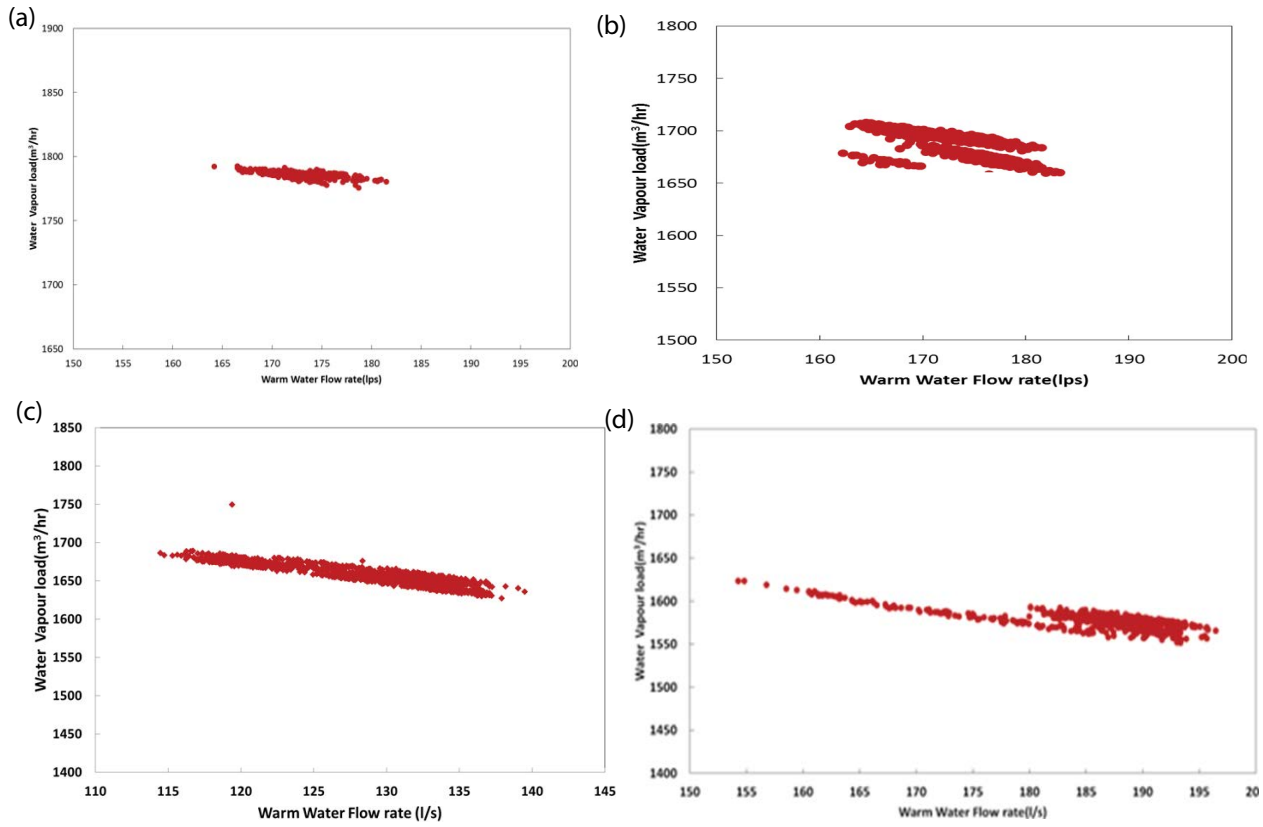

Fig. 10. Warm water flow rate vs. water vapour load with different pitch ratios are (a) 1.25, (b) 1.5, (c) 2, and (d) 3.

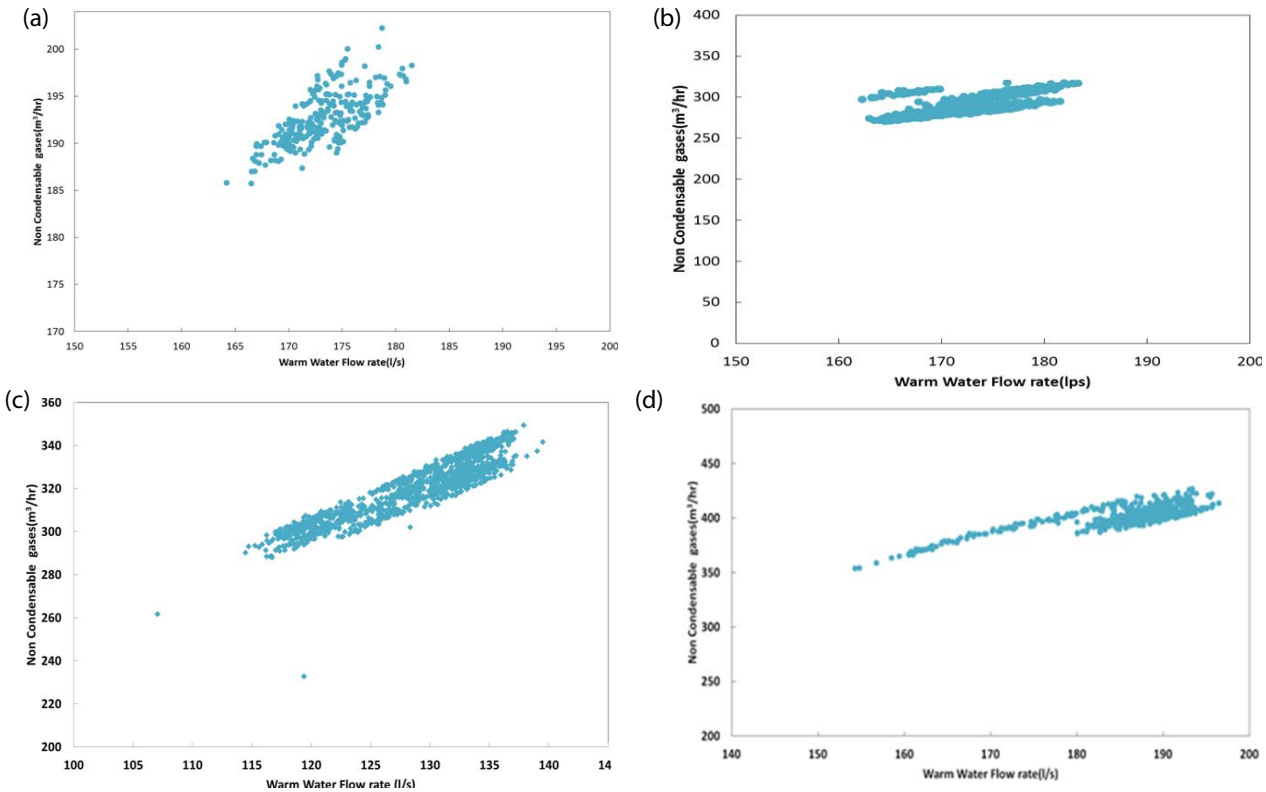

Fig. 11. Warm water flow rate vs. non-condensable gas load with different pitch ratios are (a) 1.25, (b) 1.5, (c) 2, and (d) 3.

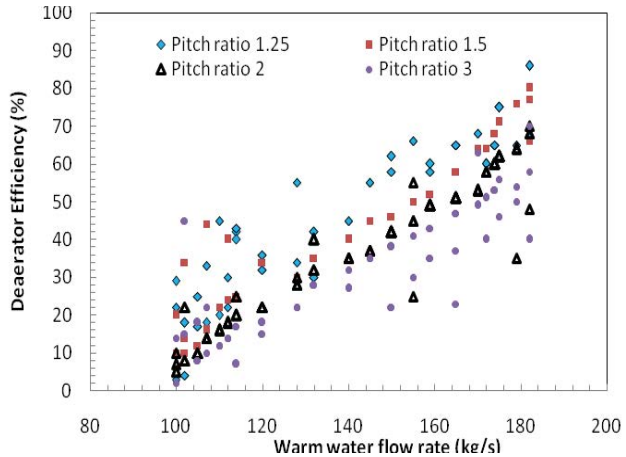

Fig. 12. Warm water flow rate vs. deaeration efficiency.

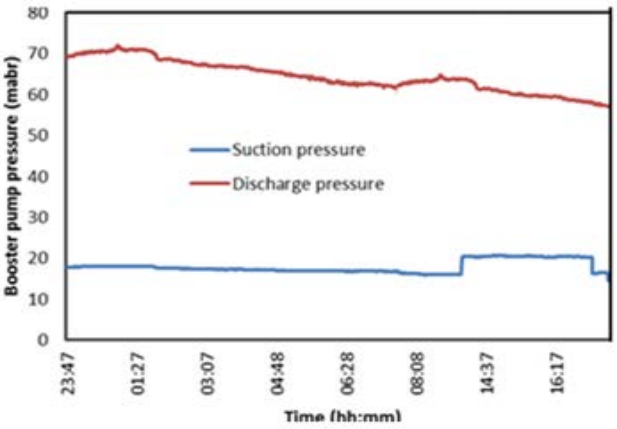

Fig. 13. Time vs. booster pressure.

and more suitable for desalination at Islands. Also, the performance ratio is found to be 0.71 only, low compared to the other desalination technologies. This could be due to the minimum operating temperature range available and single stage flash evaporation is only possible.

6. Concluding remarks

A study was carried out in Agatti LTTD plant using tube bundles of various pitch ratios (1.25, 1.5, 2, and 3) placed in the pathway of entry pipeline to deaerator for enhancing the deaeration process. Parameters such as inlet water temperature, deaerator pressure, flash chamber pressure, and inlet water flowrate, inlet pressure of the different stages of the vacuum system, fresh water production rate and the rate of water collection at the intermediate condenser of the vacuum system are collected for analysis. To determine the deaeration efficiency, a two equation model was developed. Results of analysis indicate deaeration efficiency as high as 85% and dependence of deaeration efficiency on the tide level, mass flow rate of warm water, temperature of warm water and disturbance created by the tube bundles. The air leakage load for the plant was measured to be around 0.22 kg/h against the specified limit of 4 kg/h obtained from the HEI standards. Similarly, the escape vapour load of 18 kg/h assumed as per the experience from Kavaratti Plant Data was calculated to be about 11 kg/h where the suction pressure of the roots pump dropped to as low as 14 mbar. Since the actual vacuum load is found to be lower than the designed load, running the plant by isolating a base vacuum pump of 2.2 kW capacity in the vacuum system resulted in a 16% saving in power of the vacuum system and 5% saving in the plant specific power consumption.

Table 2
Performance parameters of desalination technologies

Description	Specific electrical energy consumption (kW·h/m^3)	Performance ratio
SWRO	3.5	—
MSF	3	8
MED	2.3	12–24
LTTD	8.5	0.71

References

[1] A.K. Misra, Climate change and challenges of food and water security, Int. J. Sustainable Built Environ., 3 (2014) 153–165.
[2] M. Shatat, S.B. Riffat, Water desalination technologies utilizing conventional and renewable energy sources, Int. J. Low-Carbon Technol., 9 (2014) 1–19.
[3] H.K. Lonsdale, Recent advances in reverse osmosis membranes, Desalination, 13 (1973) 317–332.
[4] Z. Yang, Y. Zhou, Z. Feng, X. Rui, T. Zhang, Z. Zhang, A review on reverse osmosis and nanofiltration membranes for water purification, Polymers, 11 (2019) 1252, doi: 10.3390/polym11081252.
[5] M.W. Shahzad, K.C. Ng, An improved multi-evaporator adsorption desalination cycle for GCC countries, Energy Technol., (2017) 1–21, doi: 10.1002/ente.201700061.
[6] M.W. Shahzad, M. Burhan, K.C. Ng, Pushing desalination recovery to the maximum limit: membrane and thermal process integration, Desalination, 416 (2017) 54–64.
[7] I. S. Al-Mutaz, Hybrid RO MSF: a practical option for nuclear desalination, Int. J. Nucl. Desalin., 1 (2003) 47–57.
[8] S.V.S. Phani Kumar, G. Venkatesan, P. Jalihal, S. Kathiroli, Low Temperature Thermal Desalination Plants, Proceedings of Eighth ISOPE Ocean Mining Symposium, Chennai, India, Sep 20–24, 2009, OMS-2009-M09–83.
[9] R. Semiat, Y. Galerpin, Effect of non-condensable gases on heat transfer in the tower MED sea water desalination plant, Desalination, 140 (2001) 27–46.
[10] S.A. Said, I.M. Mujtaba, M. Emtir, Modelling and Simulation of the Effect of Non-condensable Gases on Heat Transfer in the MSF Desalination Plants Using PROMS Software, S. Pierucci, G. Buzzi Ferraris, Eds., Twentieth European Symposium on Computer Aided Process Engineering—ESCAPE20, Elsevier B.V., Ischia, Naple, 2010, pp. 25–30.
[11] D. Balaji, R. Abraham, M.V. Ramana Murthy, Experimental study on the vacuum load of low-temperature thermal desalination plant, Desal. Water Treat., 55 (2016) 26830–26844.
[12] C.N. Murray, J.P. Riley, T.R.S. Wilson, The solubility of gases in distilled water and sea water—I. Nitrogen, Deep Sea Res. Oceanogr. Abstr., 16 (1969) 297–310.
[13] C.N. Murray, J.P. Riley, The solubility of gases in distilled water and sea water—II. Oxygen, Deep Sea Res. Oceanogr. Abstr., 16 (1969) 311–320.
[14] N.W. Rakestraw, V.M. Emmel, The solubility of nitrogen and argon in sea water, J. Phys. Chem., 42 (1938) 1211–1215.

[15] R. Battino, T.R. Rettich, T. Tominaga, The solubility of oxygen and ozone in liquids, J. Phys. Chem., 12 (1983) 163–178.
[16] R. Battino, T.R. Rettich, T. Tominaga, The solubility of nitrogen and air in liquids, J. Phys. Chem., 13 (1984) 536–600.
[17] D.Q. Kern, Process Heat Transfer, McGraw Hill, New York, NY, 1950.
[18] Heat Exchange Institute, Standards for Steam Surface Condensers, 12th ed., 2017.
[19] B. Milow, E. Zarza, Advanced MED solar desalination plants. Configurations, costs, future — seven years of experience at the Plataforma Solar de Almeria (Spain), Desalination, 108 (1997) 51–58.
[20] A.M.K. El-Ghonemy, Performance test of a seawater multi-stage flash distillation plant: case study, Alexandria Eng. J., 57 (2018) 2401–2413.
[21] M.W. Shahzad, M. Burhan, N. Ghaffour, K.C. Ng, A multi evaporator desalination system operated with thermocline energy for future sustainability, Desalination, 435 (2018) 268–277.